THE JOURNAL OF PHYSICAL CHEMISTRY B

Article

Cite This: J. Phys. Chem. B 2018, 122, 5193−5204

pubs.acs.org/JPCB

Reorganization of Hydration Water of DPPC Multilamellar Vesicles Induced by L-Cysteine Interaction

Juan M. Arias, María E. Tuttolomondo, Sonia B. Díaz,* and Aida Ben Altabef*

INQUINOA-CONICET, Cátedra de Fisicoquímica I, Instituto de Química Física, Facultad de Bioquímica, Química y Farmacia, Universidad Nacional de Tucumán, San Lorenzo 456, T4000CAN S. M. de Tucumán, R. Argentina

Supporting Information

ABSTRACT: The aim of this study is to analyze the consequences of water redistribution on the structure and stability of phospholipid bilayers induced by cysteine (Cys). This interaction is studied with 1,2-dipalmitoyl-*sn*-glycero-3-phosphatidylcholine (DPPC) multilamellar vesicles in gel (30 °C) and liquid crystalline (50 °C) state; experimental studies were performed by means of Fourier transform infrared (FTIR) spectroscopy, Raman spectroscopy, and differential scanning calorimetry (DSC). The polar head sites of the lipid molecules to which water can bind are identified by competition with compounds that form hydrogen bonds, such as Cys. FTIR spectroscopy results revealed that there is a Cys interaction with the phospholipid head groups in the gel and liquid crystalline phases. Raman spectra were measured in the gel state. They were dominated by vibrations of the fatty acyl chains, with superposition of a few bands from the head group, and clearly showed that the S−H stretching band of Cys shifted to lower frequencies with a decrease in its force constant. DSC disclosed an overview of the behavior of the multilamellar vesicles in the working temperature range (30−50 °C) and showed how the increase of the molar ratios modified the environment of the polar head and the hydrocarbon chains. A loss of the pretransition (T_p) and an increase in the temperature of main transition (T_m) with increasing Cys/DPPC molar ratio were observed.

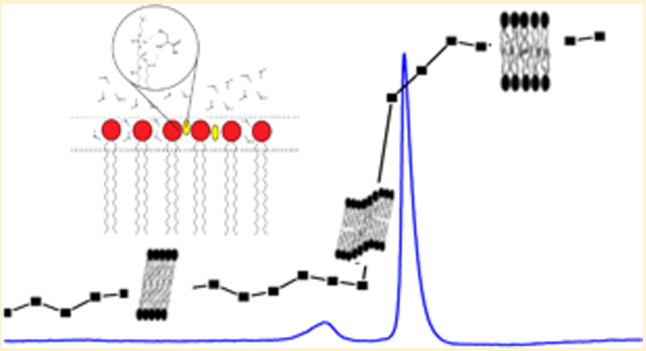

1. INTRODUCTION

The objective of this work is to study the interaction of L-cysteine (Cys) with liposomes of 1,2-dipalmitoyl-*sn*-glycero-3-phosphatidylcholine (DPPC) (Scheme 1) and characterize the role of Cys in the modification of topology and hydration of the lipid membrane. Lipids have traditionally been considered to play a fairly nonspecific role in biological systems, being rather dull compared to those assigned to proteins and genes. In fact, lipids are often tacitly assumed to constitute a less fatty material structure, which at best is organized in a membrane structure that plays the role of a passive container of the cell and an appropriate template for the important molecules of life. However, lipids are capable of self-assembling in aqueous media and can create noncovalently linked supramolecular structures with very peculiar physical properties.[1−10]

Since lipids are highly solvated by water molecules at their polar heads, the water structure on the surface of lipid membranes has a crucial role in biologically important phenomena like specific recognition of membrane-bound receptors and transmembrane substance transportation. Biological systems are subdivided by membranes, whose main structure stabilizes the lipid bilayer by hydrating phospholipids. As biological membranes are very complex systems, biomimetic systems like lipid vesicles (liposomes) have been developed to study their properties and structure.[11,12]

Cysteine is a nonessential amino acid that has a thiol group that enables it to form inter- and intrachain disulfide bonds with other cysteine residues that give it a primordial role in protein folding and functioning. Most disulfide linkages are found in proteins for export or residence on the plasma membrane.[13−17]

Scheme 1. Chemical Structures of 1,2-Dipalmitoyl-*sn*-glycero-3-phosphatidylcholine (DPPC) and L-Cysteine·HCl (Cys) Molecules Used in This Study

1,2-dipalmitoyl-sn-glycero-3-phosphatidylcholine (DPPC)

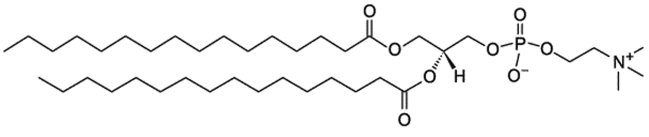

L-cysteine (Cys)

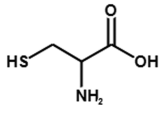

Received: February 19, 2018
Revised: April 6, 2018
Published: May 2, 2018

DOI: 10.1021/acs.jpcb.8b01721
J. Phys. Chem. B 2018, 122, 5193−5204

The free thiol is the molecular active moiety of these compounds; this group is susceptible to oxidation to give a disulfide bridge between two cysteine molecules by a covalent bond or compete with other molecules with disulfide bridges, such as glycoproteins, generating the mucolytic effect.[18]

In a previous work, we observed how it modified the region of the polar head. This interaction modifies the degree of hydration of the lipid bilayer by altering some properties of membranes, such as the transition temperature, permeability, and fluidity. The water structures in the head group region and water−hydrocarbon interface can be specific for different types of biomolecules (drugs) or different aminoacids in peptides that make water like a sensor to trigger the response of the biomembranes to external perturbations.[19,20]

We studied the Cys/DPPC interaction to analyze how Cys modifies the different phases of the lipids. Studying the specific interaction with the groups of the hydrophilic and hydrophobic regions of lipid biology and taking into account that the changes in the organization of water in the lipid interface could affect the activity or formation of some proteins, such as glycoproteins secreted by goblet cells.[21−25]

In this work, studies were performed by Fourier transform infrared (FTIR) spectroscopy and Raman spectroscopy complemented with differential scanning calorimetry (DSC) measurements to elucidate and explain the complex interaction of Cys with fully hydrated DPPC.

Raman spectroscopy was used mainly to study the behavior of the hydrophobic region of the lipid membranes. FTIR spectroscopy suffers from significant limitations in the spectral interference of solvents, the resolution, and the activity of the vibration modes of the hydrocarbon chain and proves to be inadequate for the study of the subtle molecular changes in the conformational order. Raman spectroscopy has the unique ability to provide direct information about the conformational order nondestructively and free from spectral interference.[26]

Therefore, these different approaches helped us to better understand the interaction of Cys with membrane phospholipids and how the lipid bilayer topology is affected by this.

2. EXPERIMENTAL SECTION

2.1. Lipids and Chemicals. Synthetic DPPC with purity >99%, L-cysteine, and HCl were purchased from Sigma-Aldrich Inc. (St. Louis, MO). Purity was checked by thin-layer chromatography, and lipids were used without further purification. L-Cysteine, HCl purities were checked by FTIR spectra. All other chemicals were of analytical grade, and water (Milli-Q) was employed in all of the experiments.

2.1.1. Multilamellar Vesicles (MLVs) Preparation. Multilamellar vesicles (MLVs) were prepared following Bangham's method[27] to study the Cys and DPPC interaction. The phospholipids in chloroform solutions were dried under a nitrogen stream to form a homogeneous film, which was left for 24 h under vacuum to ensure proper solvent removal. Lipids were first rehydrated and then suspended by vortexing in deionized water (Milli-Q) or D_2O and in solutions of different concentrations of Cys in H_2O (Milli-Q) or D_2O (25, 50, 75, 100, 150, and 200 mM) at 10 °C higher than the lipid-transition temperature (T_m = 41 °C). Mechanical dispersion of the hydrated lipid film was achieved under vigorous shaking for 15 min, resulting in an opalescent suspension of multilamellar vesicles (MLVs). MLV final concentration was 50 mg/mL.

2.1.2. FTIR Measurements. FTIR measurements were carried out in a PerkinElmer GX spectrophotometer provided with a DTGS detector constantly purged with dry air. Cys interaction with phospholipid head groups and hydrocarbon chains of the hydrophobic region in hydrated state was studied by dispersing the lipid and Cys/DPPC samples at different molar ratios, first in D_2O and then in H_2O. Spectra were registered in D_2O to assign the C═O stretching mode frequency (νC═O) and in H_2O to assign the antisymmetric stretching mode of the phosphate group ($\nu_a PO_2^-$). The spectra were acquired in a demountable cell with ZnSe windows for liquid samples. Cell temperature was controlled using a Peltier-type system with an accuracy of ±0.5 °C. The resolution of the equipment employed was 1 cm^{-1}. All samples were left at room temperature for 1 h before measurements. The working temperature range was 30−50 ± 0.5 °C. A total of 256 scans were made in each condition, and the spectra were analyzed using the OMNIC v.8.0 mathematical software provided by the manufacturer. Mean values of the main bands in each condition (hydrated states) were obtained from three different batches of samples. The standard deviation of the wavenumber shift calculated from this pool of data was about ±1.5 cm^{-1} in all of the conditions assayed.

The Fourier self-deconvolution algorithm was applied to define the contours of overlapping bands. Accurate wavenumbers of the center of gravity of C═O stretching component bands were obtained by using bandwidth parameters between 18 and 20 cm^{-1} and band-narrowing factors of 1.6−2.2, followed by curve fitting to obtain band intensities.

The shifts of these two populations were studied as a function of Cys concentration in gel ($L_{\beta'}$) and liquid crystalline phase (L_α). The bands of normal modes corresponding to the C═O and PO_2^- groups of the Cys/DPPC complex were assigned in comparison to the spectra of pure lipid and Cys in the aqueous solution. Cys/DPPC spectra were obtained by dispersing the lipid in Cys aqueous solutions, from which the spectrum of pure Cys aqueous solution was subtracted.

2.1.3. Raman Measurements. The vibrational Raman spectra of DPPC dispersed in a Cys aqueous solution were recorded using a confocal Thermo Scientific DXR Raman microscope equipped with a high-resolution motorized platen, a set of Olympus optical objectives, a lighting module bright-field/dark-field trinocular viewer, an Olympus camera of 2048 pixels with charge-coupled device detector, and an OMNIC Atlμs mapping software of advanced features cooled by a Peltier module. The confocal system was real, with an opening/hole matched with the point of symmetry of the excitation laser. The standard spatial resolution was better than 1 μm.

The samples were placed on gold-coated sample slides. To achieve a sufficient signal-to-noise ratio, 100 acquisitions of 5 s exposure time were accumulated for all samples. Laser power was 10 mW, and laser wavelength was 532 nm. The liquid sample was placed in a glass cuvette. All spectroscopic experiments were carried out at ambient temperature. The spectra were analyzed using the OMNIC program for dispersive Raman spectroscopy.

2.1.4. DSC Measurements. Calorimetry was performed on a PerkinElmer DSC6 differential scanning calorimeter. A scan rate of 2 °C/min was used for all samples. Sample runs were repeated at least three times to ensure reproducibility.

Data acquisition and analysis were done using data from the DSC by integrating the peak with the Pyris 6 software, provided with the set, and Origin software (Microcal). The total lipid concentrations used for the DSC analyses were about 50 mg/

DOI: 10.1021/acs.jpcb.8b01721
J. Phys. Chem. B 2018, 122, 5193−5204

mL for the Cys-phospholipid mixtures containing about 20 g H_2O/1 g lipid.[28] Samples containing Cys alone, dissolved in water (Milli-Q) at amino acid concentrations corresponding to those of the highest Cys/DPPC molar ratios studied (2.93:1), exhibited no thermal events in the 20−75 °C temperature range. This indicates that Cys does not decompose at this temperature range and that the endothermic events observed in this study arise exclusively from phase transitions of the phospholipid vesicles (Figure 1).

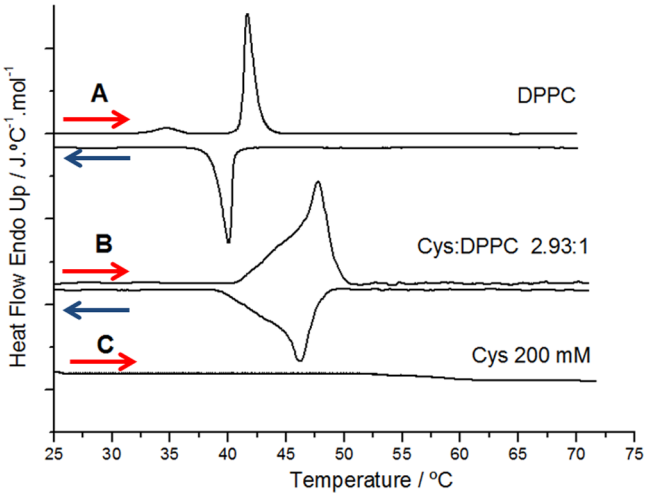

Figure 1. DSC heating (red arrow) and cooling (blue arrow) scans (scan rate, 2 °C/min) of DPPC alone and heating and cooling thermograms illustrating the effect of the exposure to high temperature on the thermotropic phase behavior of DPPC multilamellar vesicles at a Cys/DPPC molar ratio of 2.93:1. Heating scans of the 200 mM Cys solution are illustrated in A−C for comparison.

The experiments were carried out using 20 μL of sample in sealed aluminum pans. The instrument was calibrated with indium standard samples. Enthalpy changes associated to phase transition temperature of the samples (ΔH) were obtained from the DSC data by integrating the peak using the Pyris 6 software provided with the set. Entropy changes related to phase transition were finally determined with the relation $\Delta S = \Delta H/T$.

3. RESULTS AND DISCUSSION

3.1. Hydrophobic Region. *3.1.1. FTIR Measurements.* The interactions of Cys with lipid membranes of DPPC were studied by Fourier transform infrared spectroscopy. Detailed information about the molecular interactions can be obtained for hydrated liposomes in the gel (L_β) and liquid crystalline (L_α) phases. Furthermore, thermal phase transition can be monitored by following changes in the wavenumber of the CH_2 symmetric stretching. These changes increase as the acyl chains melt and the number of gauche conformers increases. In the literature,[29] the CH_2 symmetric stretching around 2850 cm^{-1} is of special significance because of its sensitivity to the changes in mobility in the conformational disorder of hydrocarbon chains.

The phase change that takes place when the hydrocarbon chains of the hydrophobic center melt during the gel transition (L_β) and liquid crystalline (L_α) phases of the phospholipids is reflected in the infrared spectra as a jump toward a higher wavenumber of the $\nu_s CH_2$ mode (Figures 2 and S1). This wavenumber jump coincides with the phospholipid transition temperature (T_m).[30,31]

The transition temperature for the pure DPPC and the mixtures with Cys can be seen in Figure 2. The value reported in the literature for the T_m of pure DPPC is 41.5 °C and presents significant changes with the increase in molar relations of Cys/DPPC. These values suggest that the interaction of cysteine with DPPC would stabilize the gel phase, causing the flow toward higher values of temperature (Table S1) for the Cys/DPPC complex at different molar ratios in D_2O and H_2O.

Wavenumber changes of symmetric and antisymmetric stretching vibrations of the CH_3 and CH_2 groups and deformation bands of the CH_2 group inside the lipid bilayer were not significant within the experimental error in the gel state. In the liquid crystalline state, we could observe a shift to

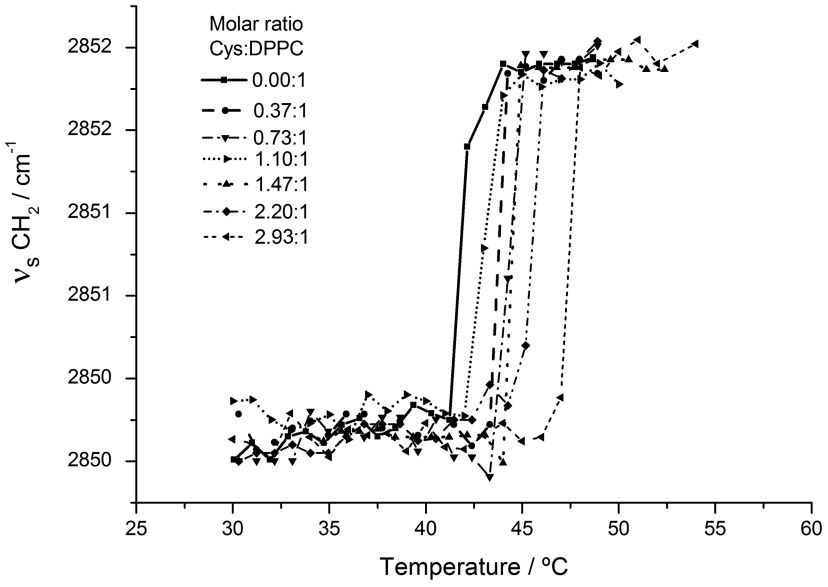

Figure 2. Changes in the wavenumber of the CH_2 symmetric stretching in Cys/DPPC (at different molar ratios) liposomes as a function of temperature.

DOI: 10.1021/acs.jpcb.8b01721
J. Phys. Chem. B 2018, 122, 5193−5204

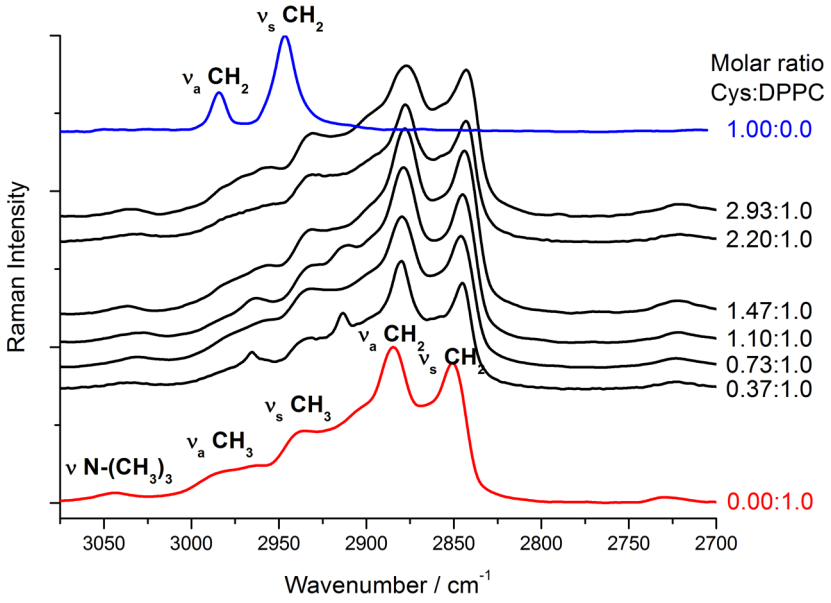

Figure 3. Peak assignment of the Raman spectrum of Cys/DPPC complex in the 3000 cm^{-1} region.

lower wavenumber in symmetric and antisymmetric stretchings of the CH_2 group (Table S2).

3.1.2. Raman Measurements. Conformational order is not easily assessed from infrared spectroscopy due to limited resolution, inactivity, weakness of major alkane vibrational modes, and poor experimental sensitivity compared to the results presented here for Raman spectroscopy. The Raman spectrum of phospholipid was dominated by vibrations of the fatty acyl chains, with superposition of a few bands from the head group.[32] Raman spectroscopy shows three regions of interest in the spectrum of pure DPPC. They are C−H stretching modes (3000−2800 cm^{-1}), CH_3 and CH_2 deformation modes (1400−1200 cm^{-1}), and a C−C stretching mode (1200−1000 cm^{-1}). The relationships between the intensities of these bands are very useful for the determinations of the different chain forms.

The symmetric and antisymmetric vibrational stretching modes of the CH_3 and CH_2 groups can be clearly seen in the region of the Raman spectrum between 3000 and 2800 cm^{-1} (Table S3 and Figure 3).

No significant changes were found in the νCH_3 frequencies of the complex with respect to pure DPPC because these displacements are within the experimental error, but we could see a shift toward lower frequencies for the CH_2 group stretching modes.

The frequencies where the $\nu_s CH_2$ and $\nu_a CH_2$ modes were observed reflect conformational order and interchain coupling; these modes were detected at 2850 and 2884 cm^{-1}, respectively, for DPPC in the gel state and decreased by 4−8 cm^{-1} in the Cys/DPPC complex, which implies a decrease in the C−H force constant of the CH_2 group. The chains would thus have greater freedom of movement.[29]

Chain coupling information can also be obtained from the intensity ratio of $\nu_s CH_3$ at 2935 cm^{-1} to $\nu_s CH_2$ at 2850 cm^{-1}. As the chains decouple (intermolecular interactions decrease), the terminal methyl groups experience increased rotational and vibrational freedom. In this case, there is no significant shift in the gel state.[26,33−35]

The high intensity ratios I_{2884}/I_{2850} ($I\nu_a CH_2/I\nu_s CH_2$) that indicate the interactions between the alkyl chains and their conformations are of interest. More specifically, these ratios can be used as an index of the disorder and order change of proportion in the conformation of the alkyl chain.

The results of the experiments carried out with increasing concentrations of the Cys/DPPC complex at 30 °C are shown in Figure 4.

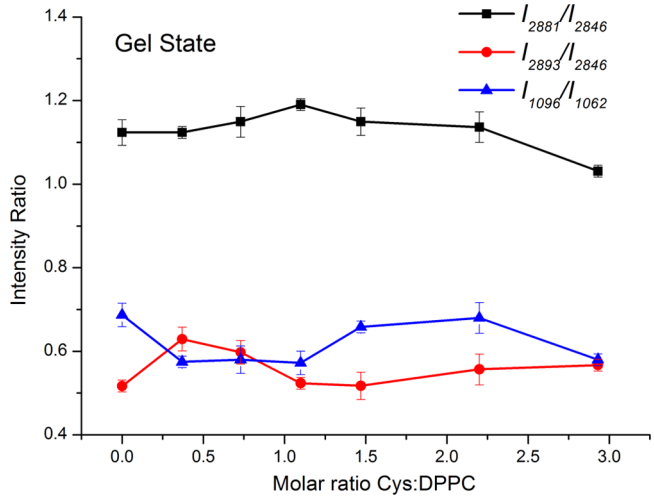

Figure 4. Intensity ratio of $\nu_a(CH_2)$ to $\nu_s(CH_2)$, ν(C−C)G to ν(C−C)T, and $\nu_s(CH_3)$ to $\nu_s(CH_2)$ as a function of the molar ratio of Cys/DPPC in gel state (30 °C).

The I_{2884}/I_{2850} intensity ratios among these vibrations are indicative of the acyl chain rotational disorder and intermolecular chain coupling. In addition, the wavenumbers of the $\nu_s CH_2$ and $\nu_a CH_2$ bands also reflect conformational order and interchain coupling (generally, wavenumber shifts toward higher values mean an increase in the decoupling of the chains). These results show that there is no increase in the intensity ratio at the molar ratios studied.[19,20,26,33]

The δCH_2 and τCH_2 bands corresponding to Cys/DPPC are shifted toward lower frequencies with respect to the pure DPPC in the Raman spectrum for all molar ratios (Table S4

DOI: 10.1021/acs.jpcb.8b01721
J. Phys. Chem. B 2018, 122, 5193−5204

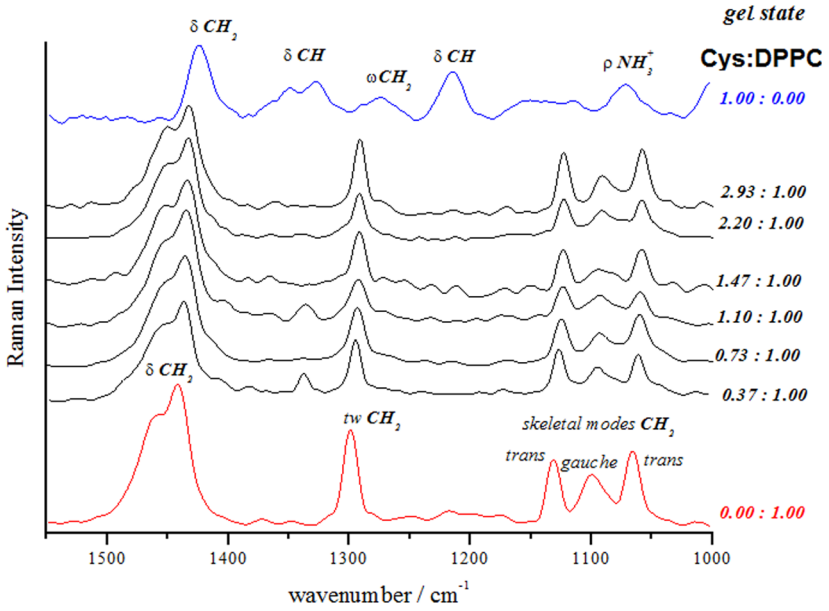

Figure 5. Raman spectra of Cys/DPPC complex (gel state, 30 °C) in the 1500−1000 cm^{-1} region.

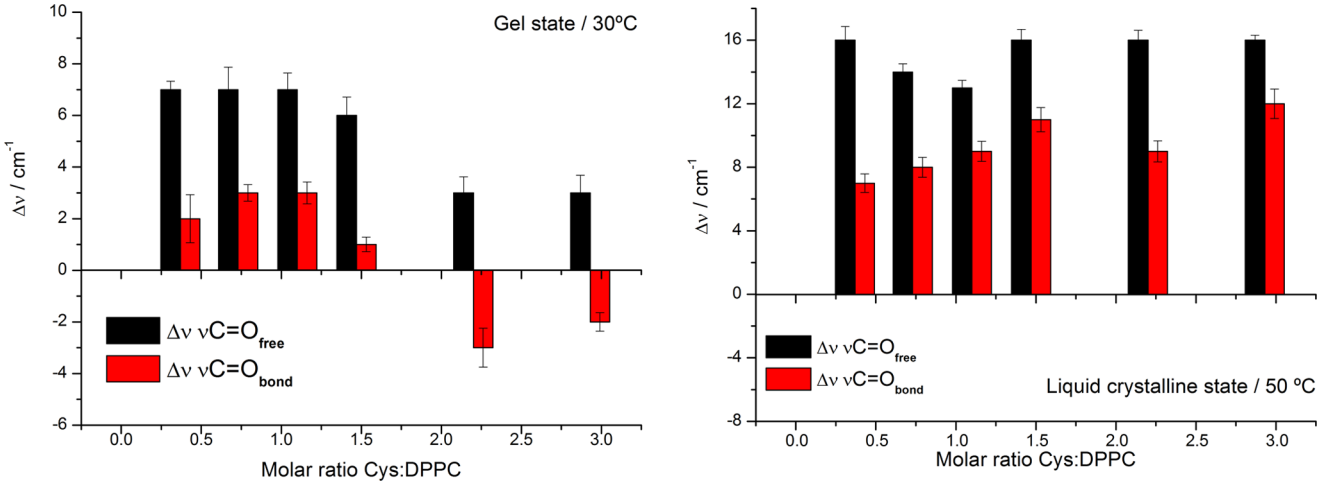

Figure 6. Wavenumber variation of the CO stretching in connection with increasing Cys/DPPC molar ratio.

and Figure 5). The frequency of these modes has also been associated with the degree of coupling between alkane chains, whereas the decoupling has been correlated with a frequency increase of this mode.[24] In this case, the Cys/DPPC interaction shows a frequency shift toward lower values, which would indicate decrease in chain order due to the presence of Cys. This behavior corresponds to an increase in the above-reported transition temperature that would indicate a stabilization of the gel phase (L_β).[29]

The region at 1300−1000 cm^{-1} includes the C−C bond stretching vibrations of the alkyl chains of the phospholipids (Figures 4 and 5 and Table S4). The band at 1066 cm^{-1} is attributed to the stretching vibration of the C−C bond for the trans conformations of the alkyl chains, whereas the band at 1099 cm^{-1} is attributed to the stretching vibration of the C−C bond for the gauche conformations of the alkyl chains. The high intensity ratios of these bands, I_{1099}/I_{1066}, also provide information about the disorder and order proportion that exists in the conformation of the alkyl chain. Both changes of band positions and intensity ratio of trans bands to gauche describe well the conformational state of alkyl chains and the gauche/trans population conformation of phospholipids.[26]

The increase in trans conformers is indicated by the increase in the value of $I[\nu(C-C)_G]/I[\nu(C-C)_T]$.[26] At all molar ratios, there were no significant changes compared to pure DDPC.

3.2. Hydrophilic DPPC or Interphase Region. *3.2.1. FTIR Measurements.* The hydrophilic region[36] may be characterized by FTIR spectra of the Cys/DPPC systems. This region is strongly dependent on the state of hydration and is susceptible to hydrogen bonding. The bands were assigned to the carbonyl and phosphate groups by comparison with pure lipids dispersed in D_2O and H_2O, respectively.

C═O Group. The band corresponding to the carbonyl group for diacyl lipids can be decomposed into at least two components that correspond to the vibrational modes of nonbonded (free) and H-bonded (bond) conformers of the C═O group. The nonbonded vibrational mode that appears at higher wavenumbers (1742−1740 cm^{-1}) was assigned to the free νC═O groups ($\nu C{=}O_{free}$), whereas the H-bonded vibrational mode that appears at lower wavenumbers (~1728 cm^{-1}) was attributed to the νC═O vibration of H-bonded

DOI: 10.1021/acs.jpcb.8b01721
J. Phys. Chem. B 2018, 122, 5193−5204

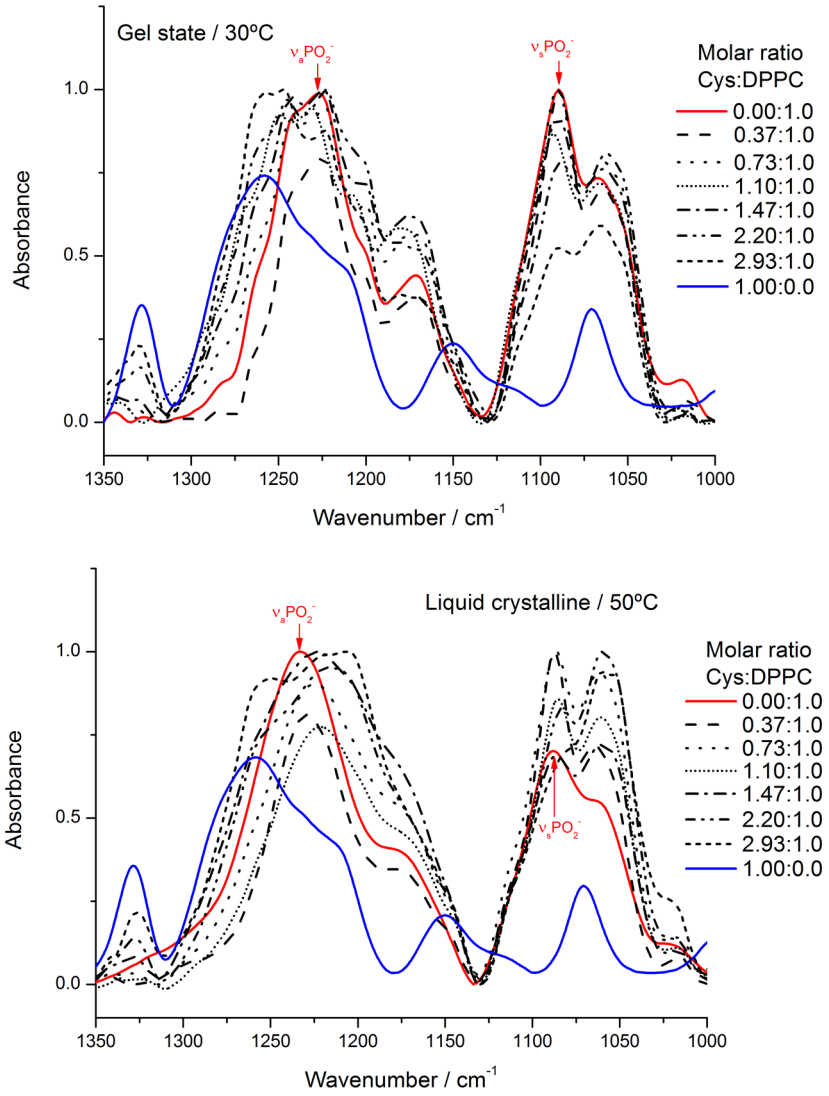

Figure 7. Effect of Cys on the position of the vibrational bands of FTIR for the PO_2^- groups in DPPC at 30 °C (gel state).

conformers (νC═O $_{bond}$).[36,37] In the FTIR and Raman spectra in the anhydrous state, a very intense band observed at 1748 cm^{-1} was assigned to the C═O stretching mode. In the water solution Raman spectrum, this band appears at about 1747 cm^{-1}.[38−41] In Figure 6, the effect of Cys at 30 °C, gel phase, and at 50 °C, liquid crystalline phase, was analyzed.

With the objective of investigating how Cys affects the region of the carbonyl groups of the lipid, the main band of the carbonyl group (located at ∼1739 cm^{-1}) was deconvolved in three components: νC═O_{bond}, νC═O_{free}, and νC═O_{Cys} (Figure S2). Assuming that the relative area of a band component is proportional to the respective conformer population, it can be concluded that the populations of C═O_{bond} and C═O_{free} conformers change upon addition of Cys. The C═O_{free} band intensity decreases with increase in molar ratio, whereas the C═O_{bond} population intensity reaches its maximum value for the 1.10:1.0 ratio in the gel state. We think this concentration would be a critical value in the interaction of amino acid with the lipid in the interphasial region of the membrane.[19] Otherwise, in the liquid crystalline state, the intensity band of the C═O_{bond} population increases with increase in the molar ratio of the complex Cys/DPPC, whereas C═O_{free} population intensity reaches its minimum value (Figure S2).

The exposure of the carbonyls to the aqueous phase is different for each phase state. This is observed by the asymmetry that the band corresponding to the carbonyl group presents when it goes from the gel to liquid crystalline state.[29]

In the literature, the wavenumbers of the component bands reported for the two populations of the carbonyl group are the nonhydrated (free) (centered at 1743 cm^{-1}) and hydrated (bond) populations (1724 cm^{-1}) in the gel state and the nonhydrated (1737 cm^{-1}) and hydrated (1722 cm^{-1}) populations in the fluid state.[36,37]

The carbonyl stretching band could be assigned to the two populations by deconvolution: νC═O_{free} (1737 cm^{-1}) and νC═O_{bond} (1729 cm^{-1}) at 30 °C, and νC═O_{free} (1729 cm^{-1}) and νC═O_{bond} (1723 cm^{-1}) at 50 °C for pure DPPC in D_2O (Figures S2 and S3 and Table S5).

A significant shift of the bands of both populations to higher wavenumbers was observed with an increase in the Cys/DPPC molar ratio at two operating temperatures: 30 °C (gel state) and 50 °C (liquid crystalline state) (Table S5).

DOI: 10.1021/acs.jpcb.8b01721
J. Phys. Chem. B 2018, 122, 5193−5204

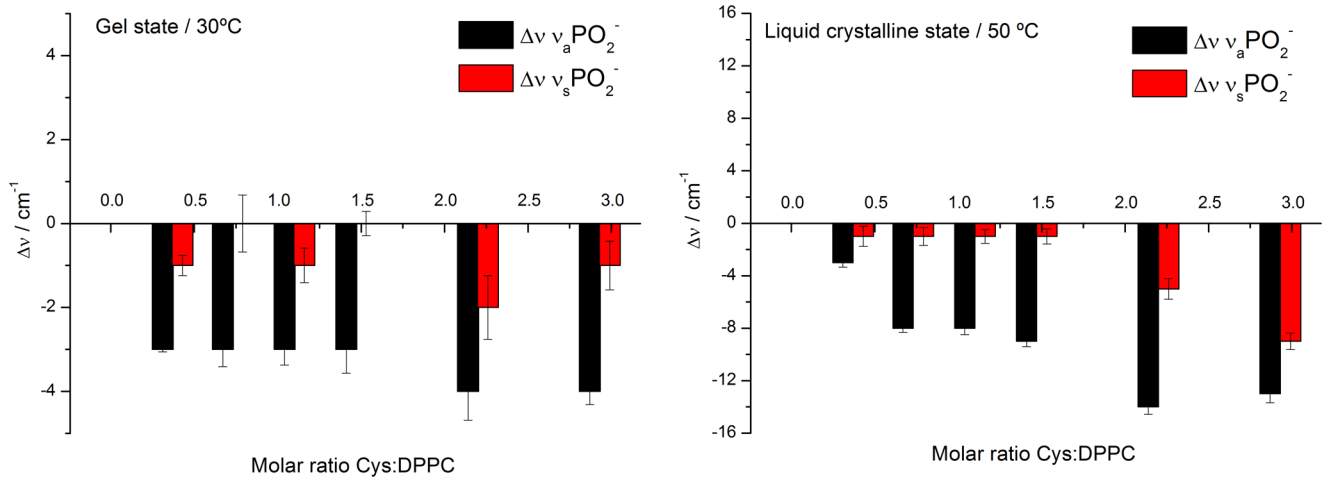

Figure 8. Infrared spectra of the symmetric and antisymmetric PO_2^- stretching vibrational modes as a function of Cys/DPPC molar ratio in gel and liquid crystalline states.

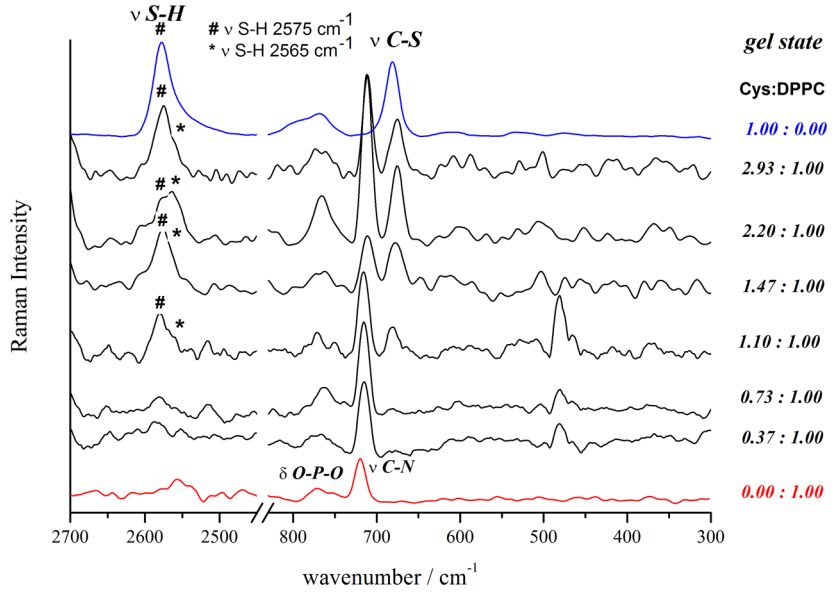

Figure 9. Raman spectrum of the DPPC, Cys, and different Cys/DPPC molar ratios in gel state at 30 °C.

This shift may occur because the polar groups are more hydrated in the fluid state, making water displacement easier for Cys. In Table S5 and Figure 6, the wavenumber displacements in connection with pure DPPC may be seen in the two states. A displacement toward higher wavenumbers with an increase in the Cys/DPPC molar ratio for both CO populations was observed in the gel state. This would imply a loss of water molecules that would be more significant for the C═O_{free} population, reaching a maximum of 7 cm^{-1} to the 1.10:1.0 molar ratio. In the liquid crystalline state, there is a wavenumber increase in the νCO_{bond} and νCO_{free} populations as the Cys/DPPC molar ratio increases in all ranges. The effects of Cys on the carbonyl group in DPPC liposomes in the liquid crystalline state (50 °C) are more notable than that observed in the gel state (50 °C). There is a maximum shift of 16 cm^{-1} for the νCO_{free} population. This behavior would suggest a displacement of hydration water molecules without subsequent formation of CO−Cys hydrogen bonds. In addition, conformational changes in the head groups may contribute to the differences observed in the C═O spectra.[19]

PO_2^- Group. Figure 7 shows the FTIR spectra corresponding to pure DPPC and Cys/DPPC hydrated liposome complexes in the region of the stretching mode of the phosphate group at 30 °C (gel state) and 50 °C (liquid crystalline state). These bands appear in the 1245−1090 cm^{-1} region.

The FTIR spectra corresponding to lyophilized and hydrated DPPC liposomes in the stretch-mode region of the phosphate group are shown in Figure S4. The PO_2^- asymmetric stretching appears at 1243 cm^{-1} like a broad and intense band with a shoulder at 1224 cm^{-1} corresponding to the wagging of CH_2.[30,31] When liposomes are hydrated, the band at 1243 cm^{-1} is observed to decrease in intensity, whereas the shoulder at 1224 cm^{-1} becomes a band of considerable intensity. It is widely accepted that the wavenumber of the PO_2^- antisymmetric stretching ($\nu_a PO_2^-$) vibration is very sensitive to lipid hydration mainly because of direct H-bonding to the phosphate-charged oxygen. Anhydrous lipid hydration displaces the band of the antisymmetric phosphate stretching to lower frequencies with increasing H-bonding.[39−45]

DOI: 10.1021/acs.jpcb.8b01721
J. Phys. Chem. B 2018, 122, 5193−5204

A shift toward lower wavenumbers was observed in Figure 8 (Table S5) when Cys was added to hydrated DPPC bilayers in the gel and liquid crystalline phases. Anhydrous lipid hydration displaces the band of the antisymmetric phosphate stretching to lower frequencies with increasing H-bonding.[36,39−43] The same trend is observed when Cys is added to hydrated DPPC bilayers, thus suggesting that the Cys−phosphate interaction is like the water/phosphate interaction in both states (Table S5). In the gel state, the change induced by Cys is more attenuated than in the fluid state, where the amino acid displaces the band of the antisymmetric phosphate stretching until 13 cm^{-1} at 2.93:1.0. The extent of the shift is an indicator of the number and strength of the H-bonds.[28] The PO_2^- symmetric stretching vibration band is slightly affected within the experimental error in both cases. However, this band is shifted 5 and 9 cm^{-1} toward lower values at 2.20:1.0 and 2.93:1.0 Cys/DPPC molar ratios, respectively.

The fluid state, although more hydrated, would facilitate water displacement by the insertion of Cys as the Cys/DPPC molar ratio increases. This would suggest that the phosphate−Cys interaction is stronger than the phosphate−water interaction. The above results simply prove that Cys would induce two effects: dehydration of the phosphate groups and subsequent formation of H-bond.

Thus, Cys molecule interaction could be affected by the different hydration levels present in the phosphate groups of both states.

3.2.2. Raman Measurements. Two bands, clearly identifiable because of the thiol group, may be seen in the Raman spectra of different Cys/DPPC molar ratios: they are the S−H and C−S stretchings. This band is sensitive to dilution.[34,46] Thus, the observed shifts of the S−H stretching band are due to S−H group interactions with some of the nucleophilic groups of the lipid membrane.[19]

S−H, C−N, and C−S Stretching Modes. The S−H stretching mode may be assigned to the band centered at 2559 cm^{-1} in the spectrum of the solid[46] by Raman spectroscopy. In solution, this band appears at a higher wavenumber (2578 cm^{-1}) because solvation of the Cl^- ion disrupts the hydrogen bonding between the SH group molecules and the chlorine atom of HCl.[19] In the gel state, this band (νS−H) appears very weak at 2575 cm^{-1} with a shoulder at 2565 cm^{-1} from the 1.10:1.0 to 2.93:1.0 molar ratio, with an increase in intensity directly related to the increase in Cys/DPPC molar ratios (Figure 9). A shift to a lower wavenumber (3 cm^{-1}) for the first band would indicate a weakening of the S−H force constant. The shoulder of these ratios is due to a lengthening of the S−H bond because of the formation of a hydrogen bond with some electronegative groups of the lipid bilayer (Figure 9).

The presence of a band at 485 cm^{-1} is observed in the Raman spectra at molar ratios 0.37:1.0, 0.73:1.0, and 1.10:1.0 with a growing intensity as the Cys/DPPC increases in molar ratio. This band is observed in the Cys−Cys dimmer and corresponds to νS−S.[46]

A small increase in the transition temperature is observed in addition to these molar ratios. If we relate this behavior with a minor frequency deviation of the symmetric stretching PO_2^- group, it may be assumed that this group could act as an oxidizing cysteine agent, resulting in an S^- anion and subsequent formation of the dimer. Only the presence of the dimer for these molar ratios may be observed due to a nonmonotonic behavior of the lipid membrane.[19,46]

An intense band corresponding to the C−S stretching mode of the Cys water solution at 681 cm^{-1} is observed for all molar ratios in the gel state in the 800−600 cm^{-1} region.[19,20,46]

The interaction of water with the choline groups ($N-(CH_3)_3$ and C−N) has been studied with different phospholipids in the literature. The peaks observed at 3042 and 720 cm^{-1} represent the stretching vibration of the $N-(CH_3)_3$ and C−N bond of the DPPC choline group in the gel state (Figure 9).

Hydrogen bonding between water and the choline group is not possible due to the positive charge of nitrogen. However, the choline group is associated with water molecules by dipole interactions,[43] and an interaction with Cys could cause a shift in the position of this vibration because of the zwitterion nature of the amino acid.

The results of the analysis in the νCH_3 region (Figure 3 and Table S3) reveal a strong interaction between the Cys and the chlorine group, with a displacement of the $\nu N-(CH_3)_3$ frequencies of about 10 cm^{-1}. The intensity changes of the peak at 715−711 cm^{-1} (Table S6) indicate a significant interaction between the choline head group and the Cys nucleophilic group, which is of the same strength independently of Cys concentration.

3.3. Differential Scanning Calorimetry Study. DSC measurements were performed to obtain a more complete picture of the phase behavior of the different Cys/DPPC molar ratios for hydrated liposomes. The parameters analyzed in the thermograms obtained were T_m, ΔH_{cal}, $\Delta T_{1/2}$, and ΔS (Table 1 and Figures S5 and S6). Phase transition temperature, generally T_m, is the one where specific heat excess reaches a maximum. For a symmetric curve, T_m represents the temperature at which the transition from the gel to liquid crystalline state is complete. The area below the DSC thermogram curve is a direct measurement of the calorimetric determination of the phase transition enthalpy, ΔH_{cal}. The cooperative unit is the ratio of van't Hoff and calorimetric enthalpies. The units of ΔH_{vH} and ΔH_{cal} are energy/cooperative unit and energy/mole unit, respectively, and the ratio $\Delta H_{vH}/\Delta H_{cal}$ gives the value of molecules per cooperative unit

$$\text{C. U.} = \Delta H_{vH}/\Delta H_{cal}$$

The larger the value of C.U., the more cooperative the phase transition. Therefore, cooperative phase transitions have larger ΔH_{vH}. The value of $\Delta T_{1/2}$ can be used as a qualitative measure of molecular cooperativity. Wider peaks correspond to less cooperative phase transitions. The use of this concept for lipid bilayers is controversial, but the value of C.U. can give a relative

Table 1. Calorimetric Parameters Analyzed for the Different Samples Studied[a]

molar ratio Cys/DPPC	T_m (°C)	ΔH_{cal} (J/mol)	$\Delta T_{1/2}$ (°C)	ΔS (J/mol K)	ΔH_{VH} (J/mol)	C.U.
0.00:1.0	41.95	74.0	0.6	0.2	12049.8	162.9
0.37:1.0	44.08	463.7	1.8	1.5	12160.9	26.2
0.73:1.0	44.49	464.3	1.5	1.5	12205.3	26.3
1.10:1.0	44.47	590.8	4.6	1.9	12260.3	20.4
1.47:1.0	47.73	781.9	4.5	2.4	12323.2	15.8
2.23:1.0	46.72	1236.9	5.0	3.9	12223.8	9.9
2.93:1.0	47.62	1805.2	4.6	5.5	13016.1	7.2

[a] T_m, transition temperature; ΔH_{cal}, transition enthalpy; $\Delta T_{1/2}$, mean height width of the principal transition; ΔS, transition entropy; ΔH_{vH}, van't Hoff enthalpies; and C.U., cooperative unit.

DOI: 10.1021/acs.jpcb.8b01721
J. Phys. Chem. B 2018, 122, 5193−5204

measure of the cooperativity of the bilayer phase transition.[47−52]

The first pronounced effect of Cys was on the phase transition behavior of DPPC. The lamellar gel (L_β) to lamellar liquid crystalline (L_α) chain melting phase transition (T_m), a cooperative phase transition, covers the conversion of a highly ordered gel state to a relatively disordered liquid crystalline bilayer. The incorporation of Cys in the phospholipid membrane altered the phase transition temperature and broadened the thermotropic peak, which indicates the occurrence of less motional freedom at higher temperatures in the presence of Cys (Figure S6).

Cooperativity or sharpness of the transition from the gel to liquid crystalline phase can also be evaluated. Phase transition sharpness is often expressed as the width of the mean height of the main transition, $\Delta T_{1/2}$. The entropic change associated to phase transition may be calculated by the following formula: $\Delta S = \Delta H_{cal}/T_m$.[48,49]

Pure DPPC thermograms and the different mixtures are shown in Figure S6, where it is possible to appreciate how the parameters analyzed change when the Cys/DPPC molar ratio increases. The pure DPPC thermogram (Figure S6) clearly shows two sharp endothermic peaks of different intensities: the lower one at 35.54 °C (T_p) and the higher one at 41.95 °C (T_m), which correspond to the pretransition ($L_{\beta'}$ to $P_{\beta'}$) and main phase transition ($P_{\beta'}$ to L_α), respectively.

The first peak presents a low transition enthalpy (9.82 J/mol) attributed to phospholipid polar head mobility, whereas the second enthalpy was assigned to hydrocarbon chain movement (Table 1).[50]

The pretransition peak at 35.54 °C (T_p) disappears with the incorporation of cysteine, whereas multicomponents appear when increasing Cys concentration. Its presence produces a significant shift toward higher temperatures in T_m from 0.37 (44.08 °C) to 2.93 (47.62 °C), and the Cys/DPPC molar ratio was observed with respect to the main transition at 41.95 °C (T_m) for pure DPPC (Figure S6 and Table 1). This would be due to Cys partition into the membrane because the lipid molecules need more energy to carry out the phase change. These results are in agreement with those observed by FTIR spectra within the experimental error (Table S1). Shifts in both directions in T_m were reported in previous studies with different drugs.[51−54]

Table 1 shows how the ΔH_{cal} value increases with increase in the Cys/DPPC molar ratio; a similar behavior was observed for the ΔS values for all of the series.

The last parameter analyzed was the mean height width of the principal transition ($\Delta T_{1/2}$), which is also very sensitive to the presence of any additives and it may indicate the changes in cooperativity. The cooperativity is inversely proportional to $\Delta T_{1/2}$. The addition of Cys broadened the calorimetric peaks and provided more asymmetric peaks (Figure S6), indicating a decrease in the transition cooperativity. These values increase compared to pure DPPC (Table 1 and Figures 1 and S6).

The polar interactions in the interphasial region of phospholipids and hydrophobic interactions between alkyl chains might be blocked by the addition of the drug. This may cause the formation of different regions in terms of interactions. As a result of these different regions, lipids do not melt at the same temperature and the transition zone broadens.[55−58]

With the Origin program, it is possible to fit the thermogram peaks and we may see that different Cys/DPPC molar ratios were formed by more than one component and, in some cases, there are up to three overlapping components. This signal overlap may be explained by the lateral phase separation, where the presence of islands or pure DPPC domains carry out a quasi-normal phase transition and there are other Cys/DPPC mixture domains that perform a phase transition at a higher temperature.[50]

4. CONCLUSIONS

In the hydrophilic region of the lipid, polar head the shifts observed in the PO_2^- asymmetric vibrations may be understood as changes in the order of water molecules in the hydration shell of the head group. The Cys effect on the phosphate group is observed: Cys−PO_2^- interaction would be higher than the H_2O−PO_2^- interaction replacing hydration water molecules more easily in the liquid crystalline state.

A water molecule displacement without later formation of a hydrogen bond is observed in the gel and liquid crystalline states in both C═O group populations in the interphase region.

The ripple phase P_β occurs just below the main transition in saturated phosphatidylcholines, and its appearance is sensitive to the addition of various biomolecules. DSC shows the transition temperature displacement toward higher temperatures, the pretransition loss, and a diminishing cooperativity in the membrane with the Cys/DPPC molar ratio increase.

Concentration-dependent and asymmetric broadening of transition peaks was seen by increasing Cys concentration. Increase in the main transition enthalpy (ΔH_{cal}) values was observed with incorporation of different molar relationships of Cys into DPPC membranes. The enthalpy change associated with the main lipid chain melting is related to molecular packing of the alkyl chain.

Our FTIR and DSC results revealed a DPPC and Cys interaction. So, an increase in both T_m and ΔH_{cal} of the gel to liquid crystalline phase transition of DPPC in the presence of Cys would indicate that stability of phospholipid bilayer in the gel phase increases because of Cys partition in the lipid.

Moreover, we observed a nonmonotonic behavior of the cysteine−lipid membrane interaction. This action could be due to the mismatch of the membrane by reordering hydration water in the lipid interphase. Thus, an energetically unfavorable penalty would result at the interphase where the two networks join. According to this value, Cys is hydrophilic ($\log P_{low}$), suggesting that the strongest Cys/DPPC interactions occur at the level of the polar head groups rather than in the membrane core. We attribute the nonmonotonic behavior of PO_2−Cys coupled with dehydration observed in the carbonyl groups to the possible formation of defects in the bilayer caused by a very high Cys/lipid ratio. The phosphate ion deprotonates the S−H site of the Cys, observing the formation of the S−S bond by the appearance of this band, since the S^- site is the nucleophilic center of this amino acid.

The bioavailabilities of the thiol (SH) and amino (NH) sites of the molecules of Cys in the membranes are comparable, since they possess the same acid strength. This is due to the inductive effect of the carboxylic group on the rest of the molecule. This effect on the esterified derivatives of Cys (methyl and ethyl cysteine) is lower, and both thiol and amino groups do not have comparable acidic strength. In this context, Cys has more probable sites for nucleophilic attacks, being its interaction more effective in the interphase region of the lipid membrane. In this way, Cys would promote an important effect decreasing the fluidity of the membrane. This results in a

DOI: 10.1021/acs.jpcb.8b01721
J. Phys. Chem. B 2018, 122, 5193−5204

progressive increase in the bandwidth of the thermogram ($\Delta T_{1/2}$) with the concentration of the Cys and phase transitions of the less cooperative lipid bilayer.

The heuristic diagram in Figure 10 shows that the Cys molecules would be accommodated in the interphase region of the lipid bilayer. The molecular dynamics simulations in a future study will also support Cys adsorption on DPPC and its specific interaction with the phosphate groups.

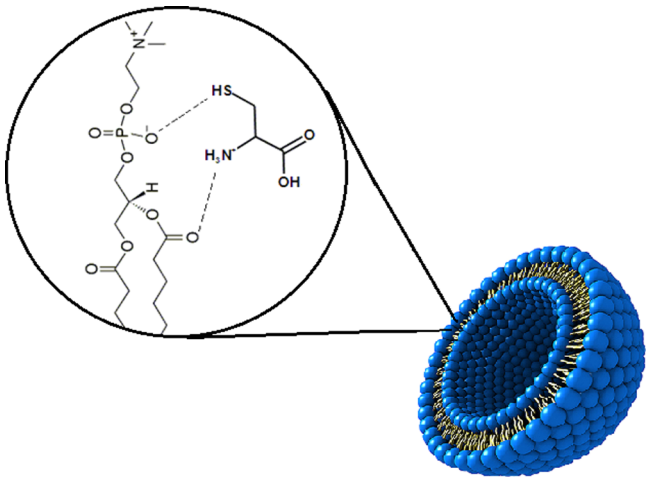

Figure 10. Heuristic diagram of the arrangement of Cys molecules in the lipid membrane.

■ ASSOCIATED CONTENT

Supporting Information

The Supporting Information is available free of charge on the ACS Publications website at DOI: 10.1021/acs.jpcb.8b01721.

Phase transition temperature for different molar ratios (Table S1); effect of Cys on the CH_2 and CH_3 vibrational bands and CH_2 deformation band (Table S2); effect of Cys on the CH_2 and CH_3 vibrational stretching bands of Cys/DPPC (Table S3); effect of Cys on the νC−C region by Raman measurements in the gel state (Table S4); C═O and PO_2^- stretching modes (Table S5); effect of Cys/DPPC on the S−H and C−S vibrational stretching bands by Raman measurements at room temperature in the gel state (Table S6); band displacements in connection with pure DPPC corresponding to symmetric and asymmetric stretchings of CH_2 group at different temperatures (Figure S1); FTIR spectral bands of carbonyl groups of Cys/DPPC (Figure S2); infrared spectra of the C═O stretching vibrational mode as a function of the Cys/DPPC molar ratio in the gel (30 °C) and liquid crystalline states (50 °C) (Figure S3); FTIR spectra corresponding to lyophilized and hydrated DPPC liposomes in the region of the stretching mode of the phosphate group (Figure S4); calorimetric parameter representation (Figure S5); and DSC thermograms of pure DPPC hydrated liposomes in different molar ratios with Cys (Figure S6) (PDF)

■ AUTHOR INFORMATION

Corresponding Authors

*E-mail: sobedi63@yahoo.com.ar (S.B.D.).

*E-mail: altabef@fbqf.unt.edu.ar. Tel: +54-0381-4311044. Fax: +54-3081-4248169 (A.B.A.).

ORCID

Aida Ben Altabef: 0000-0001-5001-5380

Notes

The authors declare no competing financial interest.

■ ACKNOWLEDGMENTS

This study was supported by funds from CONICET (PIP 002), SCAIT (PIUNT D542, Universidad Nacional de Tucumán, Tucumán, R. Argentina), and ANPCyT-PICT2013-0697. A.B.A. is a member of the Research Career of CONICET (R. Argentina). J.M.A. is a CONICET postdoc fellow of CONICET (R. Argentina).

■ REFERENCES

(1) Wolfenden, R.; Andersson, L.; Cullisand, P. M.; Southgate, C. C. B. Affinities of amino acid side chains for solvent water. *Biochemistry* **1981**, *20*, 849−855.

(2) Fauchére, J. L.; Charton, M.; Kier, L. B.; Verloopand, A.; Pliska, V. Amino acid side chain parameters for correlation studies in biology and pharmacology. *Int. J. Pept. Protein Res.* **1988**, *32*, 269−278.

(3) Radzicka, A.; Wolfenden, R. Comparing the polarities of the amino acids: side-chain distribution coefficients between the vapor phase, cyclohexane, 1-octanol, and neutral aqueous solution. *Biochemistry* **1988**, *27*, 1664−1670.

(4) Kim, A.; Szoka, F. C. Amino Acid Side-Chain Contributions to Free Energy of Transfer of Tripeptides from Water to Octanol. *Pharm. Res.* **1992**, *9*, 504−514.

(5) Hessa, T.; Kim, H.; Bihlmaier, K.; Lundin, C.; Boekel, J.; Andersson, H.; Nilsson, I.; Whiteand, S. H.; Von Heijne, G. Recognition of transmembrane helices by the endoplasmic reticulum translocon. *Nature* **2005**, *433*, 377−381.

(6) Von Heijne, G. Formation of Transmembrane Helices In Vivo-Is Hydrophobicity All that Matters. *J. Gen. Physiol.* **2007**, *129*, 353−356.

(7) Wolfenden, R. Experimental measures of amino acid hydrophobicity and the topology of transmembrane and globular proteins. *J. Gen. Physiol.* **2007**, *129*, 357−362.

(8) White, S. H. Membrane Protein Insertion: The Biology−Physics Nexus. *J. Gen. Physiol.* **2007**, *129*, 363−369.

(9) Bagatolli, L. A.; Ipsen, J. H.; Simonsen, A. C.; Mouritsen, O. G. An outlook on organization of lipids in membranes: searching for a realistic connection with the organization of biological membranes. *Prog. Lipid Res.* **2010**, *49*, 378−389.

(10) Mouritsen, O. G. Prologue: Lipidomics-A Science Beyond Stamp Collection. *Life as a Matter of Fat: The Emerging Science of Lipidomics*; Springer-Verlag: Berlin, 2005; pp 1−5.

(11) Rand, R. P.; Parsegian, V. A. Hydration forces between phospholipid bilayers. *Biochim. Biophys. Acta, Rev. Biomembr.* **1989**, *988*, 351−376.

(12) Cevc, G. Biophysical view of the role of interfaces in biomolecular recognition. *Biophys. Chem.* **1995**, *55*, 43−53.

(13) Satoh, M.; Shimada, A.; Kashiwai, A.; Saga, S.; Hosokawa, M. Differential cooperative enzymatic activities of protein disulfide isomerase family in protein folding. *Cell Stress Chaperones* **2005**, *10*, 211−220.

(14) Jessop, C. E.; et al. Oxidative Protein Folding in the Mammalian Endoplasmic Reticulum. *Biochem. Soc. Trans.* **2004**, *32*, 655−658.

(15) Álvarez, C.; Calo, L.; Romero, L. C.; García, I.; Gotor, C. An O-acetylserine (thiol) lyase homolog with L-cysteine desulfhydrase activity regulates cysteine homeostasis in Arabidopsis. *Plant Physiol.* **2010**, *152*, 656−669.

(16) Bermúdez, M. A.; Páez-Ochoa, M. A.; Gotor, C.; Romero, L. C. Arabidopsis S-sulfocysteine synthase activity is essential for chloroplast function and long-day light-dependent redox control. *Plant Cell* **2010**, *22*, 403−416.

DOI: 10.1021/acs.jpcb.8b01721
J. Phys. Chem. B 2018, 122, 5193−5204

(17) Jocelyn, P. C. *Biochemistry of the SH Group*; Academic Press Inc.: New York, 1972; pp 1−404.
(18) Servin, A. L.; Goulinet, S.; Renault, H. Pharmacokinetics of cysteine ethyl ester in rat. *Xenobiotica* **1988**, *18*, 839−847.
(19) Arias, J. M.; Tuttolomondo, M. E.; Díaz, S. B.; Ben Altabef, A. FTIR and Raman analysis of L-cysteine ethyl ester HCl interaction with dipalmitoylphosphatidylcholine in anhydrous and hydrated states. *J. Raman Spectrosc.* **2015**, *46*, 369−376.
(20) Arias, J. M.; Tuttolomondo, M. E.; Díaz, S. B.; Ben Altabef, A. Molecular view of the structural reorganization of water in DPPC multilamellar membranes induced by L-cysteine methyl ester. *J. Mol. Struct.* **2018**, *1156*, 360−368.
(21) Cole, S. J. *Mucus in Health and Disease: Regulation of the Secretory Cycle of Mucus and Serous Cell in the Human Bronchial Gland*; Elstein, M., Parke, D. K., Eds.; Plenum Press: London, 1977; pp 155−168.
(22) Yanaura, S.; Takeda, H.; Misawa, M. Behavior of mucus glycoproteins of tracheal secretory cells followings L-Cysteine methyl ester treatment. *J. Pharmacobio-Dyn.* **1982**, *5*, 603−610.
(23) Sturgess, J.; Palfrey, A. J.; Reid, L. Rheological properties of sputum. *Rheol. Acta* **1971**, *10*, 36−43.
(24) Charman, J.; Lopez-Vidriero, M. T.; Keal, E.; Reid, L. The Physical and Chemical Properties of Bronchial Secretion. *Br. J. Dis. Chest* **1974**, *68*, 215−227.
(25) Galgóczy, L.; Kovács, L.; Krizsán, K.; Papp, T.; Vágvolgyi, C. Inhibitory effects of cysteine and cysteine derivatives on germination of sporangiospores and hyphal growth of different Zygomycetes. *Mycopathologia* **2009**, *168*, 125−135.
(26) Orendorff, C. J.; Ducey, M. W.; Pemberton, J. E. Quantitative Correlation of Raman Spectral Indicators in Determining Conformational Order in Alkyl Chains. *J. Phys. Chem. A* **2002**, *106*, 6991−6998.
(27) Bangham, A. D.; Hill, M. W.; Miller, N. G. A. *Methods in Membrane Biology*; Plenum Press: New York, 1974; p 1.
(28) Popova, A. V.; Hincha, D. K. Thermotropic phase behavior and headgroup interactions of the nonbilayer lipids phosphatidylethanolamine and monogalactosyldiacylglycerol in the dry state. *BMC Biophys.* **2011**, *4*, 11.
(29) Mantsch, H. H.; McElhaney, R. N. Phospholipid phase transitions in model and biological membranes as studied by infrared spectroscopy. *Chem. Phys. Lipids* **1991**, *57*, 213−226.
(30) Casal, H. L.; Mantsch, H. H. Polymorphic phase behaviour of phospholipid membranes studied by infrared spectroscopy. *Biochim. Biophys. Acta* **1984**, *779*, 381−401.
(31) Cameron, D. G.; Casal, H. L.; Mantsch, H. H. The application of Fourier transform infrared transmission spectroscopy to the study of model and natural membranes. *J. Biochem. Biophys. Methods* **1979**, *1*, 21−26.
(32) Gaber, B. P.; Peticolas, W. L. On the quantitative interpretation of biomembrane structure by Raman Spectroscopy. *Biochim. Biophys. Acta, Biomembr.* **1977**, *465*, 260−274.
(33) Snyder, R. G.; Strauss, H. L.; Elliger, C. A. Carbon-hydrogen stretching modes and the structure of n-alkyl chains. 1. Long, disordered chains. *J. Phys. Chem.* **1982**, *86*, 5145−5150.
(34) Larsson, K.; Rand, R. P. Detection of changes in the environment of hydrocarbon chains by Raman spectroscopy and its application to lipid-protein systems. *Biochim. Biophys. Acta* **1973**, *326*, 245−255.
(35) Disalvo, E. A.; De Gier, J. Contribution of aqueous interphases to the permeability barrier of lipid bilayer for non-electrolytes. *Chem. Phys. Lipids* **1983**, *32*, 39−47.
(36) Díaz, S. B.; Biondi de López, A. C.; Disalvo, E. A. Dehydration of carbonyls and phosphates of phosphatidylcholines determines the lytic action of lysoderivatives. *Chem. Phys. Lipids* **2003**, *122*, 153−157.
(37) Blume, A.; Hübne, R. W.; Messner, G. Fourier transform infrared spectroscopy of $^{13}C{=}O$-labeled phospholipids hydrogen bonding to carbonyl groups. *Biochemistry* **1988**, *27*, 8239−8249.
(38) Díaz, S. B. Lysoderivatives Action on Lipidic Membranes in Presence of Sugars Adsorbed at the Interface. Dissertation, Universidad Nacional de Tucumán, Tucumán, R. Argentina, 2001.
(39) Lewis, R. N. A. H.; McElhaney, R. N. The structure and organization of phospholipid bilayers as revealed by infrared spectroscopy. *Chem. Phys. Lipids* **1998**, *96*, 9−21.
(40) Pohle, W.; Selle, C.; Fritzsche, H.; Binder, H. Fourier transform infrared spectroscopy as a probe for the study of the hydration of lipid self-assemblies. I. Methodology and general phenomena. *Biospectroscopy* **1998**, *4*, 267−280.
(41) Pohle, W.; Selle, C. Fourier-transform infrared spectroscopic evidence for a novel lyotropic phase transition occurring in dioleoylphosphatidylethanolamine. *Chem. Phys. Lipids* **1996**, *82*, 191−198.
(42) Arrondo, J. L. R.; Goñi, F. M.; Macarulla, J. M. Infrared spectroscopy of phosphatidylcholines in aqueous suspension a study of the phosphate group vibrations. *Biochim. Biophys. Acta* **1984**, *794*, 165−168.
(43) Jendrasiak, G. L.; Smit, R. L. The effect of the choline head group on phospholipid hydration. *Chem. Phys. Lipids* **2001**, *113*, 55−56.
(44) Frías, M. A.; Nicastro, A.; Casado, N. M. C.; Gennaro, A. M.; Díaz, S. B.; Disalvo, E. A. Arbutin blocks defects in the ripple phase of DMPC bilayers by changing carbonyl organization. *Chem. Phys. Lipids* **2007**, *147*, 22−29.
(45) Wong, P. T. T.; Mantsch, H. H. Effect of cholesterol on structural and dynamic properties of tripalmitoyl glyceride. *Chem. Phys. Lipids* **1988**, *46*, 213.
(46) López-Tobar, E.; Hernández, B.; Ghomi, M.; Sánchez-Cortes, S. Stability of the Disulfide Bond in Cystine Adsorbed on Silver and Gold Nanoparticles As Evidenced by SERS Data. *J. Phys. Chem. C* **2013**, *117*, 1531−1537.
(47) McElhaney, R. N. The use of differential scanning calorimetry and differential thermal analysis in studies of model and biological membranes. *Chem. Phys. Lipids* **1982**, *30*, 229−259.
(48) Pignatello, R. *Drug-Biomembrane Interaction Studies: The Application of Calorimetric Techniques*, 1st ed.; Woodhead Publishing, 2013; ISBN 978-1- 907568-05-3 (print).
(49) Wójtowicz, K.; Gruszecki, W. I.; Walicka, M.; Barwicz, J. Effect of amphotericin B on dipalmitoylphosphatidylcholine membranes: calorimetry, ultrasound absorption and monolayer technique studies. *Biochim. Biophys. Acta* **1998**, *1373*, 220−226.
(50) Ohline, S. M.; Campbell, M. L.; Turnbull, M. T.; Kohler, S. J. Differential Scanning Calorimetric Study of Bilayer Membrane Phase Transitions. A Biophysical Chemistry Experiment. *J. Chem. Educ.* **2001**, *78*, 1251.
(51) Paiva, J. G.; Paradiso, P.; Serroa, A. P.; Fernandes, A.; Saramago, B. Interaction of local and general anaesthetics with liposomal membrane models: A QCM-D and DSC study. *Colloids Surf., B* **2012**, *95*, 65−74.
(52) Pentak, D. Physicochemical properties of liposomes as potential anticancer drugs carriers. Interaction of etoposide and cytarabine with the membrane: Spectroscopic studies. *Spectrochim. Acta, Part A* **2014**, *122*, 451−460.
(53) Defonsi Lestard, M. E.; Díaz, S. B.; Tuttolomondo, M. E.; Sánchez Cortez, S.; Puiatti, M.; Pierini, A. B.; Ben Altabef, A. Interaction of S-methyl methanethiosulfonate with DPPC bilayer. *Spectrochim. Acta, Part A* **2012**, *97*, 479−489.
(54) Alsop, R. J.; Toppozini, L.; Marquardt, D.; Kučerka, N.; Harroun, T. A.; Rheinstädter, M. C. Aspirin inhibits formation of cholesterol rafts in fluid lipid membranes. *Biochim. Biophys. Acta* **2015**, *1848*, 805−812.
(55) Zhao, L.; Feng, S.; Kocherginsky, N.; Kostetski, I. DSC and EPR investigations on effects of cholesterol component on molecular interactions between paclitaxel and phospholipid within lipid bilayer membrane. *Int. J. Pharm.* **2007**, *338*, 258−266.
(56) Yonar, D.; Sünnetçioğlu, M. M. Spectroscopic and calorimetric studies on trazodone hydrochloride-phosphatidylcholine liposome interactions in the presence and absence of cholesterol. *Biochim. Biophys. Acta.* **2014**, *1838*, 2369−2379.
(57) Sarpietro, M. G.; Accolla, M. L.; Puglisi, G.; Castelli, F.; Montenegro, L. Idebenone loaded solid lipid nanoparticles: Calori-

DOI: 10.1021/acs.jpcb.8b01721
J. Phys. Chem. B 2018, 122, 5193−5204

metric studies on surfactant and drug loading effects. *Int. J. Pharm.* **2014**, *471*, 69−74.
(58) Yonar, D.; Sünnetçioğlu, M. M. Effect of cis-(Z)-flupentixol on DPPC membranes in the presence and absence of cholesterol. *Chem. Phys. Lipids* **2016**, *198*, 61−71.

DOI: 10.1021/acs.jpcb.8b01721
J. Phys. Chem. B 2018, 122, 5193−5204